Electric field enhanced emission from non-Coulombic traps in semiconductors

P. A. Martin, B. G. Streetman, and K. Hess
Coordinated Science Laboratory and Department of Electrical Engineering, University of Illinois at Urbana-Champaign, Urbana, Illinois 61801

(Received 12 June 1981; accepted for publication 14 August 1981)

Electric field enhancement of emission from three non-Coulombic traps has been calculated: the shielded Coulombic potential, the polarization potential, and the dipole potential. Both the Poole-Frenkel effect and phonon-assisted tunneling have been included, and both were found to be important. The field effect can be used to distinguish between these potentials on the basis of their long range character. This effect is most important in interpreting the results of capacitance transient studies of deep levels.

PACS numbers: 79.70. + q, 71.55.Fr, 72.20.Jv

I. INTRODUCTION

Deep levels in semiconductors are studied primarily by capacitance transient techniques such as deep level transient spectroscopy (DLTS).[1] These experiments detect the thermal emission of carriers from traps in the depletion region of a reverse biased junction. Thus the emission process is studied in the midst of a junction electric field which can reach 10^5–10^6 V/cm for heavily doped semiconductors. Such fields can substantially increase the emission rates being studied and must therefore be accounted for in the analysis of the experimental data.[2,3]

Models of the field-enhanced emission process have been reported in the literature, but have been limited to Coulombic potentials,[4] Dirac delta function potentials,[4] and square wells.[5] Deep levels are expected to be non-Coulombic, and therefore an extension of these calculations to other physically plausible potentials is crucial for the successful modeling of experimental results. Such an extension is also necessary if one is to use the field effect to characterize the potential well of a deep level.[4]

The purpose of this paper is to extend these calculations to include three new potentials: the shielded Coulombic or Yukawa potential, the dipole potential and the polarization potential. We will follow closely the approach of Vincent, Chantre, and Bois[4] in modeling phonon assisted tunneling. The theory of Pons and Makram-Ebeid[5] is less easily generalized for different potentials. We begin with an overview of the theory, presenting the Coulombic and square well results for reference and comparison. Results of our calculations for each of the three new potentials will then be presented.

II. OVERVIEW OF THE THEORY

There are three mechanisms of emission enhancement in an electric field: (i) the Poole-Frenkel effect, where the electron climbs over a barrier lowered by the presence of the field, (ii) pure tunneling, and (iii) phonon-assisted tunneling, where the electron absorbs thermal energy from the lattice and then tunnels through the barrier at a higher energy. These mechanisms are illustrated in Fig. 1. The pure tunneling rate between a Dirac well and the conduction band was calculated by Korol in effective mass theory.[6] Since pure tunneling becomes important only at very high electric fields ($F \sim 10^7$ V/cm), we will not consider it here.

A. Poole-Frenkel effect

The Poole-Frenkel effect is a classical mechanism in which the electron is thermally emitted over the top of a potential barrier which has been lowered by the presence of an electric field. It is based on the detailed balance expression for the emission rate without field, e_{n0}:

$$e_{n0} = e_n^\infty \exp(-E_i/k_B T), \tag{1}$$

where E_i is the ionization energy of the deep level and e_n^∞ contains the matrix elements of the transition. Any change in the barrier height is assumed to enter as a correction to E_i in Eq. (1).

The calculation was first done in a one-dimensional model by Frenkel[7] and later extended to three dimensions independently by Hartke[8] and Jonscher.[9] For a Coulombic potential in an electric field F aligned in the $-z$ direction we write the potential as

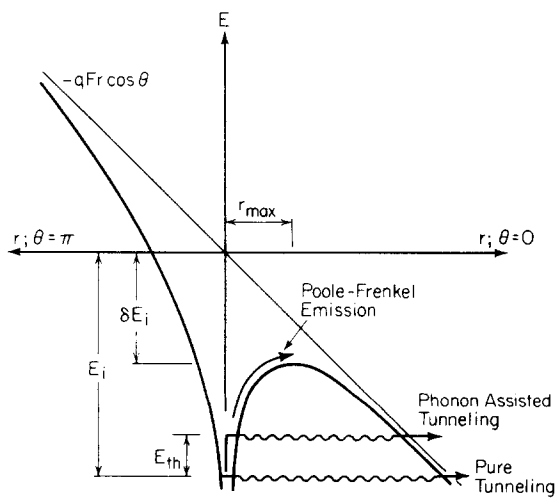

FIG. 1. Three mechanisms of field enhanced emission: Poole-Frenkel emission, phonon-assisted tunneling, and pure tunneling.

 0021-8979/81/127409-07$01.10

$$V(r) = \frac{-q^2}{4\pi\epsilon_r\epsilon_0 r} - qFr\cos\theta, \tag{2}$$

where q is the electronic charge and ϵ_r the relative dielectric constant of the host crystal. For $0 < \theta < \pi/2$ there is a well-defined potential minimum found by setting $\partial V/\partial r = 0$ at $r = r_{\max}$:

$$r_{\max} = \left(\frac{q}{4\pi\epsilon_r\epsilon_0 F\cos\theta}\right)^{1/2}. \tag{3}$$

The change in potential barrier due to the presence of the field is found by evaluating $V(r)$ at $r = r_{\max}$,

$$\delta E_i = V(r_{\max}) = -q\left(\frac{qF\cos\theta}{\pi\epsilon_r\epsilon_0}\right)^{1/2}. \tag{4}$$

Frenkel's one-dimensional result is given by setting $\theta = 0$. The emission enhancement is then

$$\frac{e_{n1}}{e_{n0}} = \exp(-\beta\delta E_i), \tag{5}$$

where $\beta = 1/k_B T$ and e_{n0} is defined in Eq. (1). The subscript 1 is used to specify a one-dimensional calculation.

The three-dimensional calculation requires an integration over θ due to the spatial variation of δE_i.

$$\frac{e_{n3}}{e_{n0}} = \frac{1}{4\pi}\left(\int_0^{2\pi} d\phi \int_0^{\pi/2} \sin\theta\, d\theta \exp[-\beta\delta E_i(\theta)] + \int_0^{2\pi} d\phi \int_{\pi/2}^{\pi} \sin\theta\, d\theta\right). \tag{6}$$

Here the subscript 3 denotes a three-dimensional calculation. The hemisphere $\pi/2 < \theta < \pi$ presents a problem in that we expect diminished emission in this direction (since here the potential is raised by the field) but there is no well-defined increase in potential height analogous to Eq. (4). We have followed Hartke in assuming that the electric field does not change the emission rate in this hemisphere.[8] Jonscher assumed no emission in this direction[9] and Hill tried to model a finite lowering of the emission rate here.[10] The difference among these treatments is small and only arises at low fields. Equation (6) can be evaluated to obtain

$$e_{n3}/e_{n0} = (1/\gamma^2)[e^\gamma(\gamma - 1) + 1] + \tfrac{1}{2}, \tag{7}$$

where

$$\gamma = (qF/\pi\epsilon_r\epsilon_0)^{1/2} q/k_B T.$$

There is a considerable difference between the one- and three-dimensional expressions (5) and (7). The one-dimensional analysis of Frenkel overestimates the field effect by calculating it only at its maximum point, at $\theta = 0$. This accounts in part for the difficulty encountered in fitting the one-dimensional theory to experimental results.[9]

The same treatment can be applied trivially to the square well. Consider a potential well of depth V_0 for $r < r_0$ and zero for $r > r_0$. This result is

$$e_{n1}/e_{n0} = \exp(\gamma), \tag{8}$$

$$e_{n3}/e_{n0} = (1/2\gamma)(e^\gamma - 1) + \tfrac{1}{2}, \tag{9}$$

$$\gamma = qFr_0/k_B T.$$

The square well is useful for many purposes, but not for modeling of the Poole-Frenkel effect. Examination of the expression for $r_{\max}$ in the Coulombic case shows that the Poole-Frenkel effect is significant for $r_{\max}$ of the order of 50–100 Å. It is precisely the long Coulombic tail of the potential which makes this an important effect at low field strengths. To model this with a square well requires values of r_0 which are grossly unrealistic for modeling anything else, such as a capture cross section. As we show below, the square well gives a reasonable phonon-assisted tunneling rate compared to other, more extended, potentials.

B. Phonon-assisted tunneling

The tunneling portion of this model is built on an expression in the WKB approximation for the transparency of the potential barrier. An electron impinging on the barrier will tunnel through with a probability

$$P = \exp\left(-\frac{(8m)^{1/2}}{\hbar}\int_{x_1}^{x_2}[V(x)]^{1/2}dx\right), \tag{10}$$

where $V(x)$ is the height of the barrier relative to the energy of the electron, m is the electron mass, and x_1 and x_2 are the points at which $V(x) = 0$.

A trapped electron can absorb a phonon and tunnel through the barrier at a higher energy where the probability P is more favorable. The probability of this composite event is

$$P_c = \exp\left(\frac{-E_{\rm th}}{k_B T}\right)\exp\left[-\frac{(8m)^{1/2}}{\hbar} \times \int_{x_1}^{x_2}\left(\frac{-q^2}{4\pi\epsilon_r\epsilon_0 x} - qFx + E_i - E_{\rm th}\right)^{1/2} dx\right], \tag{11}$$

where we have substituted the Coulombic potential in (10). E_i is again the ionization energy of the deep level and $E_{\rm th}$ is the thermal excitation energy or phonon energy. The total emission probability e_n is given by integrating (11) over all energies $E_{\rm th}$ and adding to it the Poole-Frenkel emission rate e_{n1}.

$$e_n = e_{n1} + \frac{1}{k_B T}\int_0^{E_i - \delta E_i} dE_{\rm th} P_c. \tag{12}$$

The factor $1/k_B T$ in front of the integral normalizes the integral so that the emission probability approaches 1 as F approaches infinity.[11] In this limit the emission rate is limited only by the matrix element e_n^∞ between the localized energy gap state and the conduction band states; the factor $\exp(-E_i/k_B T)$ is at high fields exactly cancelled by the emission enhancement of the field.

We can divide both sides by the zero field emission rate e_{n0} [Eq. (1)] to obtain the total relative field enhancement:

$$\frac{e_n}{e_{n0}} = \frac{e_{n1}}{e_{n0}} + \frac{e_{nt}}{e_{n0}}, \qquad \frac{e_{nt}}{e_{n0}} = \exp\left(\frac{E_i}{k_B T}\right)\frac{1}{k_B T}\int_0^{E_i - \delta E_i} dE_{\rm th} P_c. \tag{13}$$

Vincent *et al.* have an approximate form of this equation for the Coulombic potential.[4] Equation (10) gives an analytic form for the transparency of the triangular barrier of a Dirac or square well. Neglecting the Poole-Frenkel effect we have

for $z = (E_i - E_{\rm th})/k_B T$

$$\frac{e_n}{e_{n0}} = 1 + \int_0^{E_i/kT} \exp\left[z - z^{3/2}\left(\frac{4}{3}(2m)^{1/2}\frac{(k_B T)^{3/2}}{q\hbar F}\right)\right]dz. \tag{14}$$

These are one-dimensional calculations for the phonon-assisted tunneling. Thus we have used the one-dimensional Poole-Frenkel enhancement for a consistent picture, and for a comparison of the two effects. We can expect the one-dimensionality of the tunneling calculation to have the same effect as for the Poole-Frenkel effect: a substantial overestimation of the effect of the field.

It is the usual practice to use for the mass in the equations above the effective mass of the band to which emission occurs. This may seem a dubious practice since the effective mass approximation is usually invalid for deep levels. Unfortunately, if one wants to avoid the effective mass approximation, it is not enough to use the free electron mass for m; our entire approach of considering an impurity potential without any surrounding crystalline potential is equivalent to effective mass theory. Thus avoiding such an approximation requires an altogether different approach. We show below calculations for extreme values of m^*; there is a quantitative difference in the phonon-assisted tunneling rate but no qualitative difference in the importance of tunneling and of field effects in general.

Vincent *et al.* showed that, for a Coulomb potential, both the Poole-Frenkel effect and phonon-assisted tunneling are important over the field ranges of interest (e.g., 10^4–10^6 V/cm at 300 K). As shown below, we have found the same to be true for all our model potentials. The only exceptions are, of course, the square well and Dirac potentials, for which the Poole-Frenkel effect is negligible or zero.

III. YUKAWA POTENTIAL

A. Physical basis

The Yukawa, or shielded Coulombic, potential is a modification of the Coulombic potential to include screening of the charge by surrounding electrons. In the presence of an electric field the potential is

$$V(r) = \frac{-q^2}{4\pi\epsilon_r\epsilon_0 r} e^{-r/R_0} - qFr\cos\theta,$$

where R_0 is the shielding length. We will treat R_0 as an adjustable parameter. The point of maximum potential $r_{\rm max}$ is the solution to

$$\frac{q}{4\pi\epsilon_r\epsilon_0} e^{-r/R_0}\left[\frac{1}{r^2} + \frac{1}{R_0}\right] = F\cos\theta, \tag{15}$$

which must be solved numerically.

B. Poole-Frenkel effect

Some approximations are available for $r_{\rm max}$ which gives an analytical one-dimensional result for the Poole-Frenkel effect. Since these are not accompanied by analytical expressions for phonon-assisted tunneling (an effect of equal or greater importance), we feel they are of little use.

The three-dimensional Poole-Frenkel effect for the Yukawa potential is shown in Fig. 2, with the Coulomb potential result displayed for comparison. By adjusting the screening length R_0 we can achieve a continuous variation between the field dependence of a Coulomb potential and that of a Dirac potential. Note that even at $R_0 = 200$ Å the Yukawa potential dependence has not converged to that of the Coulomb potential. This underlines further the long-range character of the Poole-Frenkel effect.

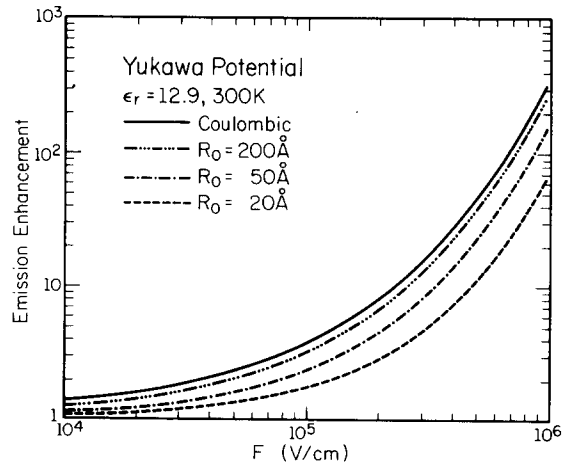

FIG. 2. Poole-Frenkel effect e_{n3}/e_{n0} for the Yukawa potential parametrized by screening length R_0.

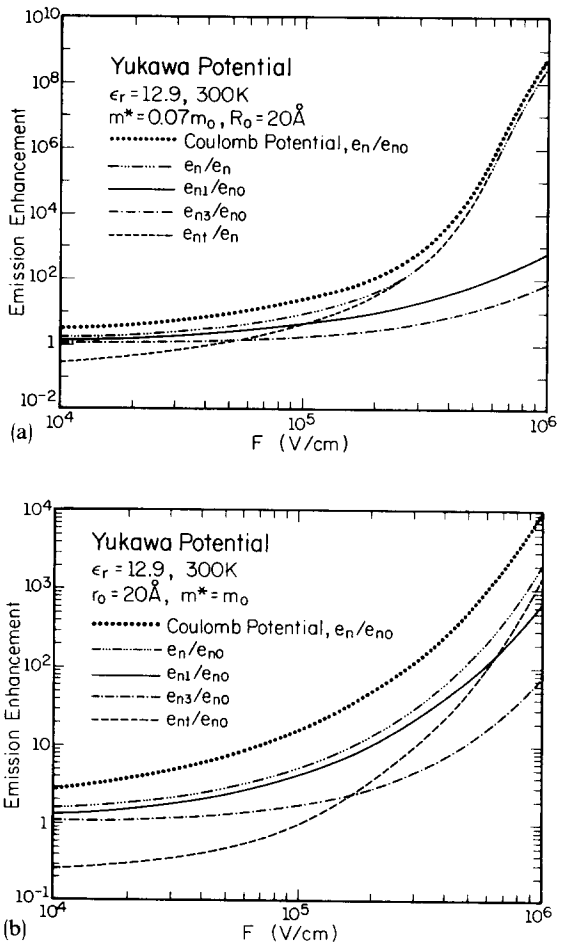

FIG. 3. Full field effect for the Yukawa potential for two values of effective mass. In each case the total field effect e_n/e_{n0} for the Coulomb potential is shown for comparison: (a) $m^* = 0.07m_0$; (b) $m^* = m_0$.

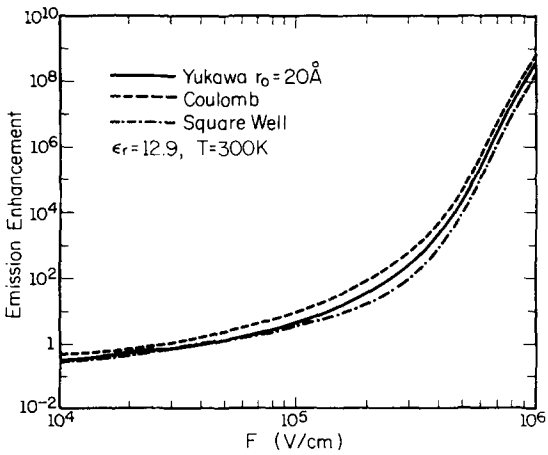

FIG. 4. Emission enhancement due to phonon-assisted tunneling e_{nl}/e_{n0} for Coulomb, Yukawa, and Dirac potentials; $m^* = 0.07m_0$.

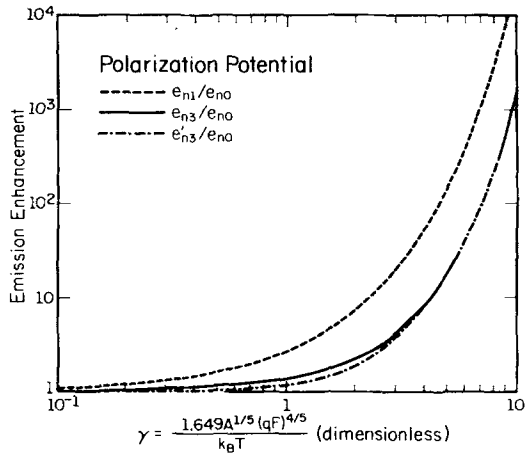

FIG. 5. Poole-Frenkel effect for the polarization potential in one- and three-dimensional models. e'_{n3}/e_{n0} includes a diminished emission rate in the reverse direction.

C. Phonon-assisted tunneling

The full field effect calculation is shown in Fig. 3 for two values of effective mass: $m^* = 0.07m_0$ and $m^* = m_0$. In each case the Coulombic result is shown for comparison. This change in the effective mass changes the tunneling calculation quantitatively but does not affect the importance of phonon-assisted tunneling, or of field effects in general. Figure 4 shows the phonon-assisted tunneling rate e_{nl}/e_{n0} compared for the Coulomb, Yukawa, and Dirac wells. (The square well shows the same phonon-assisted tunneling rate as the Dirac well.) As expected, those potentials with greater spatial extent show a greater field dependence. The emission enhancement among these potentials varies by, at most, an order of magnitude.

IV. POLARIZATION POTENTIAL

A. Physical basis

Lax used a polarization potential to model capture of electrons and holes by neutral impurities.[12] Tasch and Sah used this potential to model the observed field dependence of Au in Si.[2] The potential is of the form

$$V(r) = -A/r^4 \qquad (16)$$

$$A = q^2\alpha/8\pi\epsilon_0\epsilon_r^2,$$

where α is the polarizability of the neutral impurity atom and ϵ_r the relative dielectric constant of the host crystal. Lax estimated $A = 2\times10^{-31}$ eV cm^4 for Si:Au.

B. Poole-Frenkel effect

With an electric field in the $-z$ direction, the total potential is

$$V(r) = (-A/r^4) - qFr\cos\theta, \qquad (17)$$

giving a maximum in potential barrier height at

$$r_{\max} = (4A/qF\cos\theta)^{1/5} \qquad (18)$$

and a reduction in barrier height of

$$\delta E_i = -(5\times4^{-4/5})A^{1/5}(qF\cos\theta)^{4/5}$$
$$= -1.649A^{1/5}(qF\cos\theta)^{4/5} \qquad (19)$$

in the range $0 < \theta < \pi/2$. The one-dimensional Poole-Frenkel emission enhancement is given by

$$e_{n1}/e_{n0} = \exp\gamma \qquad (20)$$

and the three-dimensional case by

$$\frac{e_{n3}}{e_{n0}} = \frac{1}{2}\left(1 + \frac{5}{4}\int_0^1 d\tau\,\tau^{1/4}\exp\gamma\tau\right),$$

$$\gamma = 1.649A^{1/5}(qF)^{4/5}/k_BT. \qquad (21)$$

Using Hill's technique for dealing with the raising of the barrier in the reverse direction,[10] we assign an increase in barrier height for $\pi/2 < \theta < \pi$ equal to the corresponding lowering of the barrier $\theta' = \theta + \pi$. This results in

$$\frac{e'_{n3}}{e_{n0}} = \frac{5}{4}\int_0^1 d\tau\,\tau^{1/4}\cosh(\gamma\tau). \qquad (22)$$

While these integrals cannot be solved analytically, their numerical evaluation results in universal curves as functions of γ which give the Poole-Frenkel effect for any combination of parameters. These curves are shown in Fig. 5.

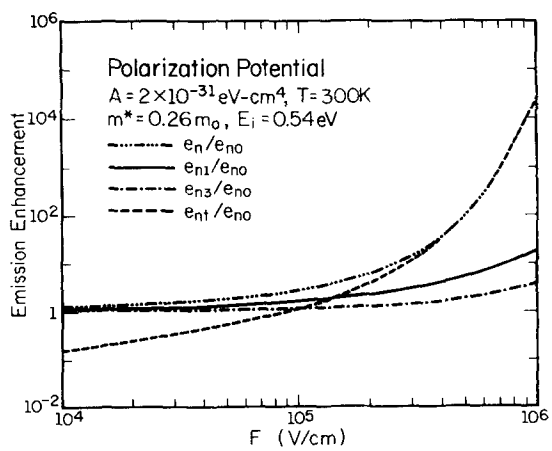

FIG. 6. Full field effect for the polarization potential.

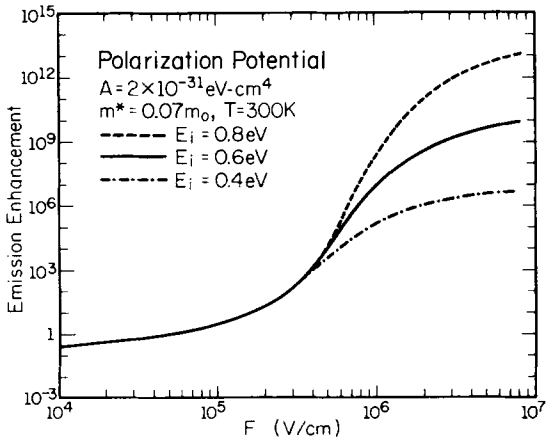

FIG. 7. Emission enhancement due to phonon-assisted tunneling e_{nt}/e_{n0} for the polarization potential, parametrized by ionization energy E_i.

C. Phonon-assisted tunneling

The emission enhancement due to phonon-assisted tunneling is shown in Fig. 6 with the complete field effect. This calculation represents the Au level in silicon at 0.54 eV below the conduction band edge. We use the estimate of Lax for $A = 2\times 10^{-31}$ eV cm^4 for this system.

The ionization energy is not a critical parameter for the phonon assisted tunneling enhancement except at very high field strengths. This is demonstrated in Fig. 7, which shows the phonon-assisted tunneling enhancement for three values of E_i. At low field strengths the tunneling which predominates is through a region near the top of the potential well, which is common to wells of any depth. The dependence on E_i begins only at higher fields where the enhancement factor approaches its limiting value of $\exp(E_i/k_B T)$. Vincent[11] showed this to be true for the Coulombic potential; we have found it true for all of our model potentials. These comments are, of course, limited to field enhancement (e_{nt}/e_{n0}); the emission rate itself (e_{nt}) will be more strongly dependent on E_i.

V. DIPOLE POTENTIAL

A. Physical basis

A complex of two oppositely charged centers, each with charge magnitude of Zq, is represented by a dipole potential

$$V(r) = \frac{q\hat{r}\cdot\mathbf{P}}{4\pi\epsilon_r\epsilon_0 r^2}, \tag{23}$$

with a dipole moment given by

$$P = |\mathbf{P}| = Z|q|R, \tag{24}$$

where R is the distance separating the two charge centers. We define the $\hat{z}$ axis to lie along $\mathbf{P}$ and in spherical coordinates the potential becomes

$$V(r) = \frac{-qP\cos\theta}{4\pi\epsilon_r\epsilon_0 r^2} \tag{25}$$

B. Poole-Frenkel effect

We now consider the potential in an externally applied electric field. We let $\mathbf{F}$ form an angle θ_F with the z axis and define the $\theta = 0$ plane to be that containing $\mathbf{F}$ and $\mathbf{z}$. The orientation of the field and dipole moment is shown in Fig. 8. The complete potential then becomes

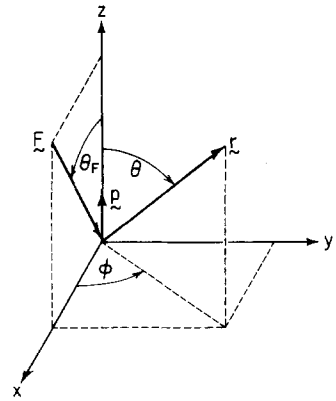

FIG. 8. Orientation of the dipole potential with dipole moment P in an electric field $\mathbf{F}$.

$$V(r) = \frac{-qP\cos\theta}{4\pi\epsilon_r\epsilon_0 r^2} - qrF\sin\theta_F\sin\theta\cos\phi - qrF\cos\theta_F\cos\theta. \tag{26}$$

In the hemisphere $\cos\theta < 0$, this potential forms an infinite repulsive barrier to the emission of electrons. Quantum mechanically, we can expect some emission in this direction, but such a process lies beyond the limiting assumptions of the Poole-Frenkel emission mechanism. For the present calculation we assume no emission takes place, with or without field, into this hemisphere. We also assume, as usual, that the emission rate is unchanged in the region in which the field raises the potential barrier.

Solving for the point of maximum potential as before, we have

$$r_{\max} = \left(\frac{(P/2\pi\epsilon_r\epsilon_0)\cos\theta}{F\sin\theta_F\sin\theta\cos\phi + F\cos\theta_F\cos\theta}\right)^{1/3}, \tag{27}$$

and the change in barrier height is given by

$$\delta E_i = -(3\times 2^{-2/3})\left(\frac{P}{4\pi\epsilon_r\epsilon_0}\cos\theta\right)^{1/3} \times (F\sin\theta_F\sin\theta\cos\phi + F\cos\theta_F\cos\theta)^{2/3}. \tag{28}$$

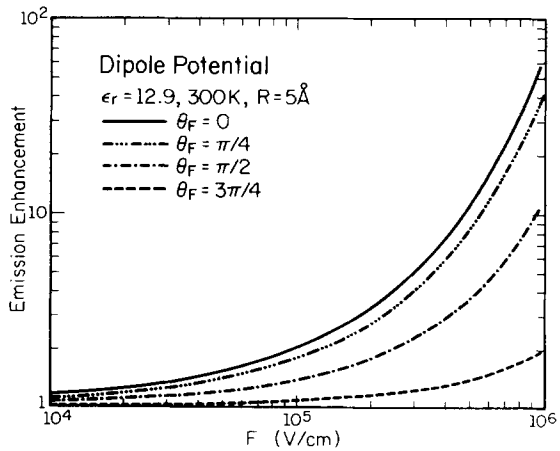

FIG. 9. Poole-Frenkel effect e_{n3}/e_{n0} for the dipole potential for four orientations of electric field.

Unlike the other potentials studied in this work, the dipole potential experiences a barrier lowering which is ϕ-dependent. The three-dimensional Poole-Frenkel effect is thus given by a double integral which in general has no analytic solution. Because of the problem of fixing the limits of integration, the integral falls into two cases.

Case 1: $0 < \theta_F \leqslant \frac{1}{2}\pi$.

The barrier is lowered for

$$-\pi/2 < \phi \leqslant \pi/2$$

and for

$$\pi/2 < \phi < 3\pi/2,$$

$$0 < \theta < \tan^{-1}(-\cot\theta_F/\cos\phi),$$

$$\frac{e_{n3}}{e_{n0}} = \frac{1}{2\pi}\int_{-\pi/2}^{\pi/2} d\phi \int_0^{\pi/2} \sin\theta\, d\theta \exp[-\beta\delta E_i(\theta,\phi)] + \frac{1}{2\pi}\int_{\pi/2}^{3\pi/2} d\phi \int_0^{\tan^{-1}(-\cot\theta_F/\cos\phi)} \sin\theta\, d\theta \exp[-\beta\delta E_i(\theta,\phi)] + \frac{1}{2\pi}\int_{\pi/2}^{3\pi/2} d\phi \left[1+\left(\frac{\cot\theta_F}{\cos\phi}\right)^2\right]^{-1/2}. \quad (29)$$

Case 2: $\pi/2 < \theta_F < \pi$

The barrier is raised for

$$\pi/2 < \phi < 3\pi/2$$

and for

$$\pi/2 < \phi < \pi/2,$$

$$0 < \theta < \tan^{-1}(-\cot\theta_F/\cos\phi).$$

The barrier is lowered for

$$\pi/2 < \phi < \pi/2,$$

$$\tan^{-1}(-\cot\theta_F/\cos\phi) < \theta < \pi/2,$$

$$\frac{e_{n3}}{e_{n0}} = 1 - \frac{1}{2\pi}\int_{-\pi/2}^{\pi/2} d\phi \left[1+\left(\frac{\cot\theta_F}{\cos\phi}\right)^2\right]^{1/2} + \frac{1}{2\pi}\int_{-\pi/2}^{\pi/2} d\phi \int_{\tan^{-1}\left(\frac{-\cot\theta_F}{\cos\phi}\right)}^{\pi/2} \sin\theta \times \exp[-\beta\delta E_i(\theta,\phi)]\, d\theta \quad (30)$$

In the case $\theta_F = 0$, the θ dependence disappears and the problem can be solved analytically. The barrier lowering simplifies to

$$\delta E_i = -1.9\left(\frac{P}{4\pi\epsilon_r\epsilon_0}\right)^{1/3} F^{2/3}\cos\theta, \quad (31)$$

and the Poole-Frenkel emission enhancement is given by

$$e_{n3}/e_{n0} = \frac{1}{\gamma}(e^{\gamma}-1), \quad (32)$$

where

$$\gamma = 1.9\left(\frac{P}{4\pi\epsilon_r\epsilon_0}\right)^{1/3} F^{2/3}/k_B T.$$

The three-dimensional result is shown for several field orientations in Fig. 9.

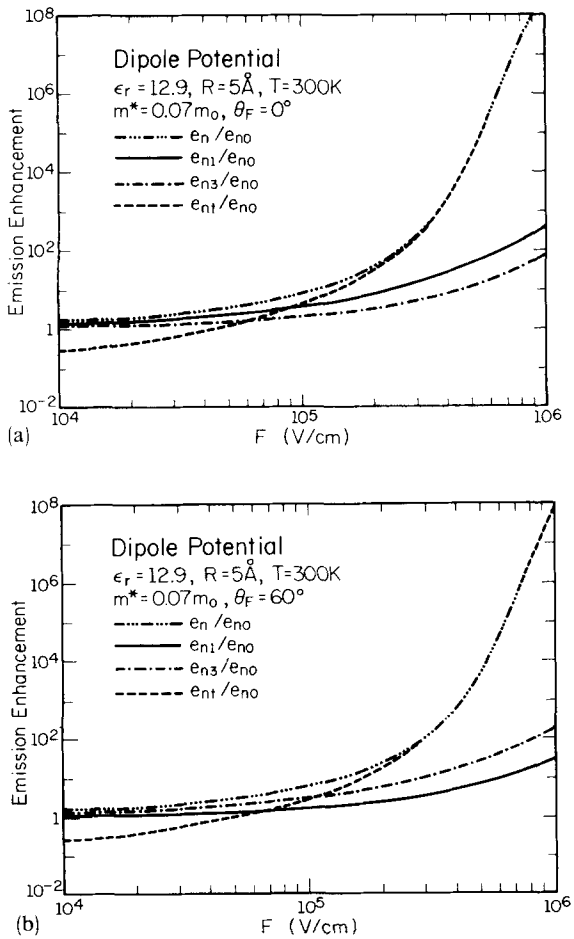

FIG. 10. Full field effect for the dipole potential for two orientations of electric field: (a) $\theta_F = 0°$; (b) $\theta_F = 60°$.

C. Phonon-assisted tunneling

The one-dimensional analysis necessary for tunneling is also complicated by the reduced symmetry of the dipole potential. For all other potentials studied here, the one-dimensional analysis was done at $\theta = 0$, where the Poole-Frenkel barrier lowering was greatest. For the dipole potential, however, the maximum barrier lowering occurs at some θ_m such that $0 < \theta_m < \theta_F$, and at $\phi = 0$, as determined from Eq. (28). Differentiating the expression for δE_i with respect to θ at $\phi = 0$ and setting the result equal to zero we find a solution for θ_m:

$$\theta_m = \tan^{-1}\left(\frac{(8+\cos^2\theta_F)^{1/2} - 3\cos\theta_F}{2\sin\theta_F}\right).$$

The phonon assisted tunneling and one-dimensional Poole-Frenkel effect are calculated at this value of θ. The results are shown in Fig. 10.

VI. DISCUSSION

The starting point of the work described in this paper was the idea that the field dependence of the emission rates might be useful to identify deep traps. Indeed we saw that the various potentials exhibit quite different field dependences. However, the field dependence is always dominated by the behavior of the potential far from the central cell. A powerful clarification of deep levels can therefore hardly be achieved with this method. One should be able, however, to distinguish roughly between Coulombic, short range, dipole, and polarization potentials.

In the case of a few deep levels in GaAs, the field dependence of the emission rates has been successfully modeled by available theories.[4,13] Such efforts were not successful, however, for the EL2 level in GaAs,[4] where a strongly anisotropic field effect was later observed.[14] While the interpretation of the observed anisotropy is still far from clear,[15] it is most likely due to a similar anisotropy in the defect potential. The dipole potential is one candidate which deserves consideration, although other, similarly anisotropic potentials are equally likely at this point. A rigorous determination must await more detailed experiments. Field dependence measurements of other levels are not yet available.

The major relevance of field dependent emission rates is therefore the evaluation of transient capacitance methods. In the light of the above formulas, this evaluation is only straightforward if the continuum approximation of the *p-n* junction (or Schottkey barrier) built-in field is appropriate. In view of the highly nonlinear character of the formulas presented above, it is highly unlikely that such a case exists. The distance of the deep level to the next shallow doping impurity will enter the emission behavior, and pairing, etc., can be of utmost importance. It is clear that under such circumstances the continuum approximation of the built in field is poor and an accurate determination of the energy of a deep level using the above formulas can be expected only if the field dependence is weak.

This makes the study of deep levels in alloys using transient capacitance methods difficult. In addition to the "shallow dopant field," high fields exist in alloys due to compositional disorder and/or cluster formation.[15]

The actual value of this "alloy field" depends on details such as cluster size, etc., which are hard to estimate. Furthermore, in many instances the approximation of the alloy effect on the deep level by a microscopic fluctuating field will be poor.

It seems to be a fact, however, that the field dependence of emission rates is much stronger in ternary alloys than in binary compounds or elemental semiconductors. This in turn indicates that the field dependence itself is easier to study in the alloy where the external fields can be rather low.

ACKNOWLEDGMENTS

This work was supported by the Office of Naval Research. We are grateful for fruitful discussions with J. D. Dow, A. Bhattacharyya, and J. Blaisdell, and to G. Vincent for providing a copy of his thesis. We also acknowledge the help of the MACSYMA computer system- a product of the Mathlab group of the Laboratory for Computer Science at MIT. The work of the Mathlab group is supported in part by the United States Energy Research and Development Administration and by the National Aeronautics and Space Administration.

[1]D. V. Lang, J. Appl. Phys. **45**, 3023 (1974).
[2]A. F. Tasch, Jr. and C. T. Sah, Phys. Rev. B **1**, 800 (1970).
[3]D. V. Lang, J. Appl. Phys. **45**, 3014 (1974).
[4]G. Vincent, A. Chantre, and D. Bois, J. Appl. Phys. **50**, 5484 (1979).
[5]D. Pons and S. Makram-Ebeid, J. Phys. Theor. Appl. **40**, 1161 (1979).
[6]E. N. Korol, Sov. Phys. Solid State **19**, 1327 (1977).
[7]J. Frenkel, Phys. Rev. **54**, 647 (1938).
[8]J. L. Hartke, J. Appl. Phys. **39**, 4871 (1968).
[9]A. K. Jonscher, Thin Solid Films **1**, 213 (1967).
[10]R. M. Hill, Philos. Mag. **23**, 59 (1971).
[11]G. Vincent, thesis, Lyon 1978.
[12]M. Lax, Phys. Rev. **119**, 1502 (1960).
[13]S. Makram-Ebeid, Appl. Phys. Lett. **37**, 464 (1980).
[14]A. Mircea and A. Mitonneau, J. Phys. Theor. Appl. **40**, L31 (1979).
[15]S. Makram-Ebeid, Proc. Mater. Res. Soc. Symp., 1980, Vol. 2, *Defects in Semiconductors*, edited by J. Narayan and T. Y. Tan (North Holland, New York, 1980), p. 495.
[16]N. Holonyak, Jr., W. D. Laidig, B. A. Vojak, K. Hess, J. J. Coleman, P. D. Dapkus, and J. Bardeen, Phys. Rev. Lett. **45**, 1703 (1980).